

Conformational Flexibility of C8-Phenoxyguanine Adducts in Deoxydinucleoside Monophosphates

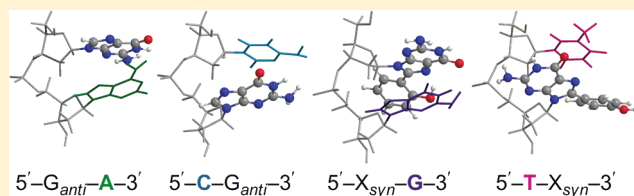
Andrea L. Millen,[†] Breanne L. Kamenz,^{†,§} Fern M. V. Leavens,^{†,§} Richard A. Manderville,[‡] and Stacey D. Wetmore^{*,†}

[†]Department of Chemistry, University of Lethbridge, 4401 University Drive, Lethbridge, Alberta, Canada T1K 3M4

[‡]Department of Chemistry, University of Guelph, Guelph, Ontario, Canada N1G 2W1

 Supporting Information

ABSTRACT: M06-2X/6-31G(d,p) is used to calculate the structure of all natural deoxydinucleoside monophosphates with G in the 5' or 3' position, the *anti* or *syn* conformation, and each natural (A, C, G, T) base in the corresponding flanking position. When the *ortho* or *para* C8-phenoxy-2'-deoxyguanosine (C8-phenoxy-dG) adduct replaces G in each model, there is little change in the relative base–base orientation or backbone conformation. However, the orientation of the C8-phenoxy group can be characterized according to the position (5' versus 3'), conformation (*anti* versus *syn*), and isomer (*ortho* versus *para*) of damage. Although the degree of coplanarity between the phenoxy ring and G base in the *ortho* adduct is highly affected by the sequence since the hydroxyl group can interact with neighboring bases, the *para* adduct generally does not exhibit discrete interactions with flanking bases. For both adducts, steric clashes between the phenoxy group and the backbone or flanking base destabilize the *anti* conformation preferred by the natural nucleotide and thereby result in a clear preference for the *syn* conformation regardless of the sequence or position. This contrasts the conclusions drawn from smaller (nucleoside, nucleotide) models previously used in the literature, which stresses the importance of using models that address the steric constraints present due to the surrounding environment. Since replication errors for other C8-dG bulky adducts have been linked to a preference for the *syn* conformation, our findings provide insight into the possible mutagenicity of phenolic adducts.



INTRODUCTION

DNA can be damaged in a variety of ways, often resulting in the loss of genetic information.¹ For example, oxidation,^{2–4} alkylation,^{5–7} and deamination^{8,9} are common processes that alter nucleobase recognition during replication.¹⁰ Indeed, oxidation of guanine (G) to 8-oxoguanine leads to G → T (thymine) transversion mutations,³ while deamination of cytosine (C) to uracil (U) leads to C → T transition mutations.⁸ Similarly, addition of aryl radical species to DNA results in bulky adducts (addition products) that have varying mutagenic consequences.^{11–13} Specifically, C8-arylamine,^{14–19} polycyclic aromatic hydrocarbon,^{20–25} and C8-phenoxy-based^{26–33} G adducts have all been linked to different types of cancers.¹ The formation mechanism of some C8 adducts has been extensively researched in recent years. For example, C8-arylamine adducts have been studied both computationally and experimentally.^{34–42} Regardless, the mechanism by which these species induce carcinogenesis is less understood²¹ compared with that of damage inflicted by, for example, 8-oxoguanine and uracil.^{43,44}

The most stable geometric configuration of bulky DNA-damaged products plays an integral role in dictating their mutagenic nature,⁴⁵ where the relative population of the *anti* and *syn* conformations is particularly important.²¹ Specifically, natural 2'-deoxyguanosine (dG) preferentially adopts an *anti* conformation, which directs the Watson–Crick hydrogen-bonding face toward

the neighboring strand (Figure 1a, left) and results in selective binding to C upon DNA replication. However, the *syn* conformation (Figure 1b,c, right) of many bulky DNA adducts is favored.^{21,45–48} Adopting this conformation prevents Watson–Crick hydrogen-bonding with the natural complementary base and thereby leads to base substitution or frameshift mutations if left unrepaired.^{49–51} Alternatively, some bulky adducts adopt both the *anti* and *syn* conformations, which contributes to an even more complicated mutagenic profile.^{15,52–55}

Due to the correlation between the *anti/syn* preference of DNA-damaged products and their mutagenic mechanism, our group has been studying the bulky carbon-bonded products of phenoxy radical attack at the C8 position in guanine. Specifically, we have been using a combined computational and experimental approach to assess the favored geometric conformation(s),^{56–58} as well as the hydrogen-bonding properties,⁵⁹ of the *ortho* and *para* C8-phenoxy-2'-deoxyguanosine adducts (*o*-PhOH-dG and *p*-PhOH-dG). Our previous work reveals that the *anti* and *syn* conformations of the dG nucleoside adducts are nearly thermoneutral,⁵⁶ while nucleoside 5'-monophosphate adducts have a stronger preference for the *anti* conformation.⁵⁶ However,

Received: June 18, 2011

Revised: September 23, 2011

Published: September 26, 2011

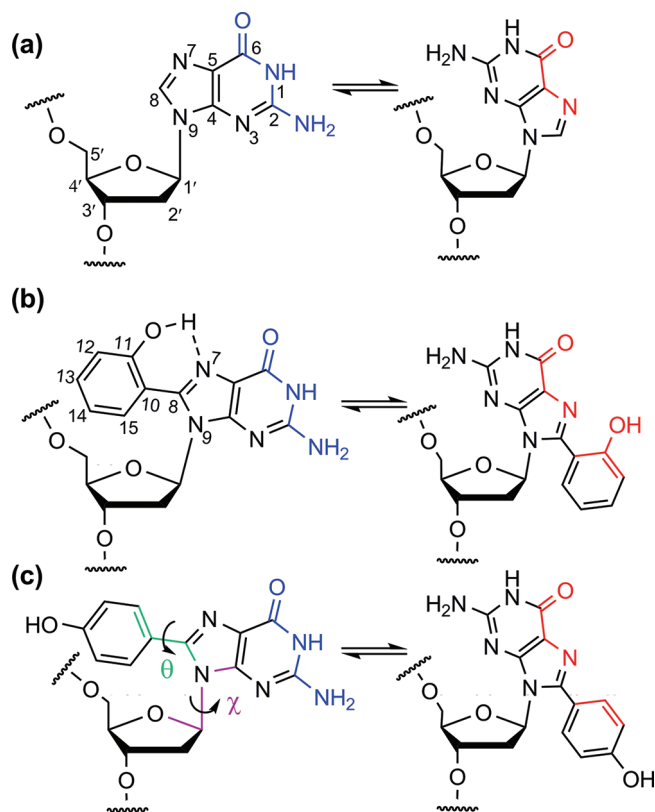


Figure 1. Structure and chemical numbering of (a) natural 2'-deoxyguanosine (dG) and (b) the *ortho* (*o*-PhOH-dG) and (c) *para* (*p*-PhOH-dG) C8-phenoxyl-dG adducts considered in the present work. The dihedral angle χ ($\angle(\text{O4}'\text{C1}'\text{N9C4})$ for purines, purple) defines the glycosidic bond conformation to be *anti* (left, Watson–Crick bonding faces in blue) when $\chi = 180^\circ \pm 90^\circ$ or *syn* (right, Hoogsteen bonding faces in red) when $\chi = 0^\circ \pm 90^\circ$. θ ($\angle(\text{N9C8C10C11})$, green) defines the degree of twist between the nucleobase and the bulky substituent ($\theta = 0^\circ$ or 180° represents a planar structure).

the calculated *anti/syn* energy difference is still small, which suggests that both conformations may exist within DNA helices.⁵⁶ Therefore, increasing the model size may further clarify the conformational preference of the adducts since other factors within duplexes may be able to preferentially stabilize one conformation.⁵⁹ For example, strong hydrogen-bonding interactions with a particular natural base can preferentially stabilize a *syn* mismatch.^{55,60–62} In addition, the identity of the flanking bases has influenced the preferred conformation of other bulky C8 adducts.^{15,17,63–65}

The present study expands the computational models of *o*-PhOH-dG and *p*-PhOH-dG previously investigated by considering damaged deoxydinucleoside monophosphates (Figure 2) with adducts in either the 5' or 3' position and each of the four natural nucleobases (A (adenine), C, G, T) in the corresponding flanking position. We are particularly interested in a deoxydinucleoside monophosphate since this is the smallest model that accounts for intrastrand stacking, which may affect the *anti/syn* ratio for bulky adducts due to interactions between the bulky substituent and the backbone or neighboring bases.¹⁷ Furthermore, since similar models have been successfully used to investigate the sequence dependence of the conformations of natural B-DNA,^{66–68} a deoxydinucleoside monophosphate model will afford information about structures relevant to the DNA

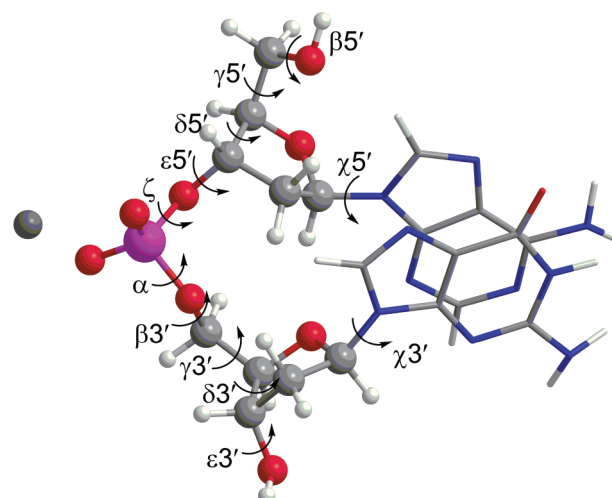


Figure 2. Representative deoxydinucleoside monophosphate with a sodium counterion phosphate model considered in the present study and definition of important backbone dihedral angles ($\beta 5' = \angle(\text{HO5}'\text{C5}'\text{C4}')$, $\gamma = \angle(\text{O5}'\text{C5}'\text{C4}'\text{C3}')$, $\delta = \angle(\text{C5}'\text{C4}'\text{C3}'\text{O3}')$, $\epsilon 5' = \angle(\text{C4}'\text{C3}'\text{O3}'\text{P})$, $\zeta = \angle(\text{C3}'\text{O3}'\text{PO5}')$, $\alpha = \angle(\text{O3}'\text{PO5}'\text{C5}')$, $\beta 3' = \angle(\text{PO5}'\text{C5}'\text{C4}')$, and $\epsilon 3' = \angle(\text{C4}'\text{C3}'\text{O3}'\text{H})$). The glycosidic bond dihedral angles ($\chi 5'$ and $\chi 3'$) are equal to $\angle(\text{O4}'\text{C1}'\text{N9C4})$ for purine-containing and $\angle(\text{O4}'\text{C1}'\text{N1C2})$ for pyrimidine-containing nucleotides.

environment. Indeed, the effects of sequence context on the preferred *anti/syn* conformation of other bulky C8 adducts (2-aminofluorene-C8-dG (dG-AF) and 2-(acetyl amino)fluorene-C8-dG (dG-AAF)) were similarly studied using deoxydinucleoside monophosphate models^{53,69} prior to investigation of the adducts in larger sequences.^{70–74} The aforementioned studies on natural strands and those containing other bulky adducts suggest that this work will also permit the dissection of sequence effects on the conformational preference of the phenoxyl adducts, which are currently unknown. In addition to broadening our knowledge of the effects of sequence context on the conformational preference of the adducts, the information gained from this work will be useful for identifying sequence contexts with interesting base–base interactions for study in future large-scale molecular dynamics simulations of phenoxyl adducts incorporated into DNA helices.

COMPUTATIONAL DETAILS

Deoxydinucleoside monophosphate models were generated for base sequences with the natural, *o*- or *p*-C8-phenoxylguanine nucleobase in the 5' or 3' position and each of the natural bases in the corresponding flanking position (see, for example, Figure 2). Initially, the structure of the dApdG sequence was built from a central dinucleotide in a well-studied experimental crystal structure of a DNA dodecamer (PDB code 436D)⁷⁵ and optimized according to the methodology outlined below. Subsequently, the nucleobase sequence was altered to generate all natural sequences examined in this work. Corresponding damaged sequences were generated by adding the phenoxyl substituent to G and setting the sugar pucker and the θ ($\angle(\text{N9C8C10C11})$, Figure 1) dihedral angle, which controls the relative orientation of the bulky group and nucleobase, to the values previously calculated using a 2'-deoxyguanosine 5'-monophosphate model.⁵⁶ Subsequently, the natural or damaged guanine nucleobase was rotated about

the glycosidic bond to generate the corresponding *syn* structures (Figure 1).

The computational literature studying DNA structure and reactions has used a variety of different phosphate models in attempts to describe the complicated environment of DNA helices.^{66,76–87} Although anionic and neutral (protonated) phosphate models have been widely used, our previous work shows that neither model accurately reproduces the *anti/syn* stability of the natural dG 5'-monophosphate nucleotide.⁵⁶ Therefore, the present study uses a counterion phosphate model where a sodium ion is equidistant between two oxygen atoms in the phosphate backbone. This model also predicts the correct *anti/syn* preference for dG in a nucleotide model⁵⁶ and successfully reproduces the average values of B-DNA backbone dihedral angles in natural deoxydinucleoside monophosphates.⁶⁶ Additionally, this model likely provides a more accurate representation of the DNA environment, where counterions are common in solution.⁶⁶

Each possible sequence of the deoxydinucleoside monophosphate with the sodium counterion phosphate model was optimized with M06-2X/6-31G(d,p) in water ($\epsilon = 78$) using the IEF-PCM formalism.⁸⁸ Although our previously published work used B3LYP to study the conformational properties of the corresponding nucleoside and nucleotide models,^{56,57} this functional incorrectly accounts for dispersion interactions.⁸⁹ Therefore, B3LYP is not a viable choice for studying deoxydinucleoside monophosphates, which include stacking interactions. In contrast, M06-2X was designed in part to yield more accurate noncovalent interactions that contain significant dispersion contributions, as well as reliable thermochemical data.⁹⁰ The effects of the (bulk) environment were taken into account during the optimization step since our previous work concluded this approach is necessary to successfully optimize the biologically relevant *syn* conformation of 2'-deoxyguanosine 5'-monophosphate.⁵⁶ Although a relatively small basis set was implemented in the present work due to the size of our models, the chosen functional, basis set, and environment combination is further justified by the good agreement between the structure of natural deoxydinucleoside monophosphate models and B-DNA (see the discussion below).

All geometric variables were freely optimized with the exception of the $\beta 5'$ ($\angle(\text{HOC}5'\text{C}4')$, Figure 2) dihedral angle, which was constrained to 180° to prevent interactions with the nucleobase that are non-native to DNA helices. Frequency calculations were also performed on all structures. Reported relative energies were obtained from M06-2X/6-311+G(2df,p) single-point calculations and include scaled (0.9580)⁹¹ zero-point vibrational energy corrections. All calculations were performed with Gaussian 09.⁹²

RESULTS AND DISCUSSION

The present work considers the effects of bulky C8-phenoxy substituents on the structure, and particularly the *anti/syn* conformational preference, of deoxydinucleoside monophosphate sequences containing natural 2'-deoxyguanosine. All possible nucleobase sequences are considered with dG, *o*-PhOH-dG, or *p*-PhOH-dG located at the 5' or 3' position and one of the four natural bases in the corresponding flanking position. The discussion of the optimized structures will focus on the relative base–base orientation and the backbone conformation since bulky adducts have been shown to affect both of these geometric variables.^{47,48,69} As done in previous work,^{67,68} the relative base–base orientation will be assessed by measuring the

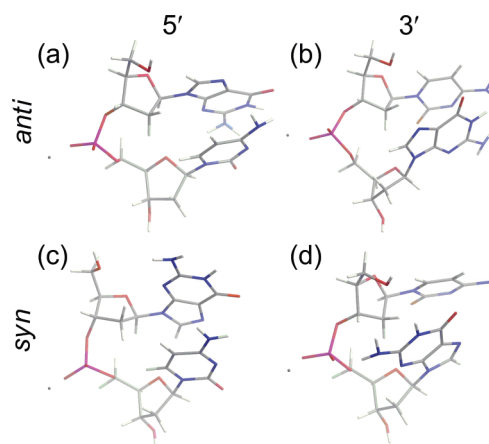


Figure 3. M06-2X/6-31G(d,p) structure of natural dGpdC (a, c) and dCpdG (b, d) deoxydinucleoside monophosphates with dG in the *anti* (a, b) or *syn* (c, d) conformation.

angle (designated as φ) between base planes (defined as the mean plane generated using endocyclic heavy atoms). φ combines the values of tilt and roll commonly used to describe relative nucleobase arrangements in DNA double helices,⁹³ where $\varphi = 0^\circ$ indicates a parallel stacked base–base orientation. The backbone conformation will be compared to that of natural DNA⁹⁴ by analyzing important torsional angles along the sugar–phosphate backbone (Figure 2). Due to the large number of sequences considered and the number of interesting geometric features of DNA strands, select examples are used to illustrate our major findings. In the discussion below, the structure and *anti/syn* conformational preference for natural dG sequences will be initially considered, and subsequently, the effects of DNA damage on these parameters will be examined for the *o*-PhOH-dG and *p*-PhOH-dG adducts.

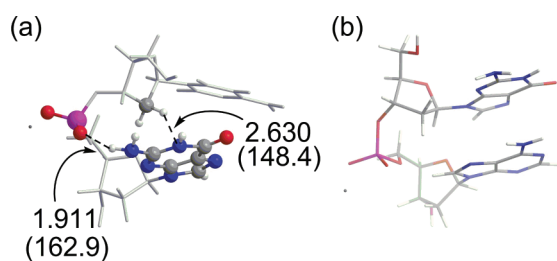
Natural Deoxydinucleoside Monophosphates. Figure 3 displays representative structures of the natural deoxydinucleoside monophosphate optimized in the present work. In all sequences, the nucleobases remain in an orientation relevant to natural DNA helices and do not exhibit significant distortion compared to crystal structure data.⁹⁴ More specifically, despite a small degree of tilt between the bases in some of the deoxydinucleoside monophosphates (Table 1), stacked base arrangements are obtained for all sequences with 2'-deoxyguanosine in the *anti* conformation regardless of whether located in the 5' or 3' position (see, for example, Figures 3 a,b). Indeed, as previously reported for a deoxydinucleoside monophosphate described using a counterion phosphate model,⁶⁷ φ is generally less than 12° except for sequences with a pyrimidine in the 5' position ($\varphi \approx 20\text{--}25^\circ$, Table 1). Although highly parallel base–base conformations are observed when dG adopts the *syn* conformation in the 5' position ($1^\circ < \varphi < 10^\circ$), a greater degree of tilt ($\varphi = 16\text{--}27^\circ$) is found for *syn*-dG in the 3' position (Table 1). The tilted base–base arrangements observed in the latter structures maximize interactions between the guanine nucleobase and both the phosphate ($\text{N}2\text{--H}\cdots\text{O}$) and sugar ($\text{C}2'\text{--H}\cdots\pi$) groups (Figure 4a). Regardless, the relative base–base orientations reported here closely resemble those found in B-DNA helices, which exhibit variations in stacked base–base arrangements.⁶⁸

Since bulky DNA adducts may significantly affect the local structure of the DNA backbone,⁴⁸ it is particularly important to analyze the backbone orientation in the optimized natural

Table 1. Tilt Angles Defining the Base–Base Orientation (φ , deg) and Relative Arrangement of the Phenoxy and Guanine Rings (θ , deg) for Deoxydinucleoside Monophosphates Containing Natural dG or a (*ortho* or *para*) C8-Phenoxy Adduct^{a,b}

position	conformation	base	cytosine		thymine		adenine		guanine	
			φ	θ	φ	θ	φ	θ	φ	θ
5'	<i>anti</i>	G	10.2		5.9		12.7		11.2	
		<i>p</i> -PhOH-G	15.9	144.6	15.5	150.3	2.5	148.4	22.1	144.7
		<i>o</i> -PhOH-G	18.4	149.6	18.5	156.4	21.9	147.4	13.7	140.7
	<i>syn</i>	G	1.6		7.2		1.8		9.2	
		<i>p</i> -PhOH-G	7.6	217.7	10.2	215.9	4.1	218.1	14.2	223.3
		<i>o</i> -PhOH-G	11.5	222.7	12.0	212.7	17.2	237.5	14.3	211.3
3'	<i>anti</i>	G	20.3		24.8		9.2		11.2	
		<i>p</i> -PhOH-G	21.0	146.4	23.1	139.9	18.6	127.4	28.3	142.6
		<i>o</i> -PhOH-G	18.8	155.7	20.4	156.3	9.4	157.6	10.8	159.9
	<i>syn</i>	G	26.1		24.3		16.3		16.5	
		<i>p</i> -PhOH-G	27.3	219.8	24.0	212.2	25.5	207.4	22.6	212.6
		<i>o</i> -PhOH-G	25.4	204.0	23.8	204.4	24.3	201.4	22.4	204.5

^a M06-2X/6-31G(d,p)-optimized geometries. φ is the degree of tilt between the base planes defined by the mean plane generated using endocyclic heavy atoms. θ (\angle (N9C8C10C11)) defines the degree of twist between the nucleobase and the bulky substituent ($\theta = 0^\circ$ or 180° represents a planar structure, Figure 1). ^b For the *ortho* adduct nucleotide model, $\theta = 159.7^\circ$ (*anti*) or 203.4° (*syn*). For the *para* adduct nucleotide model, $\theta = 148.6^\circ$ (*anti*) or 217.1° (*syn*). See ref 47.

**Figure 4.** M06-2X/6-31G(d,p) structures (hydrogen bond distances in angstroms, angles in degrees) for *syn*-dG in the (a) 3' or (b) 5' position.

sequences. This will allow us to ensure our model is accurate and permit reliable comparisons to the bulky adducts for which crystal structure data are scarce. Due to the number of configurations and backbone torsion angles considered (Figure 2), Table 2 displays the average values across all sequences according to the position (5' or 3') of *anti*- or *syn*-dG, while data for individual structures are provided in the Supporting Information (Table S1). The *anti* χ values fall within the experimental averages obtained from crystal structures of B-DNA⁹⁴ and are also very close to the values calculated using a nucleotide model ($\chi = 243.9^\circ$).⁵⁶ The remainder of the calculated dihedral angles are also in good agreement with those observed in B-DNA regardless of the location of the *anti*-dG conformation (Table 2) and resemble previous results obtained using a similar computational approach.^{66,67} The χ values of the *syn* conformation vary (by $4\text{--}17^\circ$) from those reported for the nucleotide model ($\chi = 67.9^\circ$).⁵⁶ The remaining backbone torsion angles for deoxydinucleoside monophosphates containing *syn*-dG at the 3' position deviate by less than 13° from the average crystal structure values for *anti*-dG (Table 2), which suggests an *anti*/*syn* conversion has a small impact on the structure of the backbone. However, larger deviations from the average experimental backbone conformation occur when *syn*-dG is in the 5' position, where the variation is generally less than 10° , but can be up to $21\text{--}26^\circ$ (see $\epsilon 5'$ and $\delta 3'$, Table 2). The larger deviations for strands with *syn*-dG in the 5'

position suggest that the backbone may undergo distortion to accommodate the *syn* conformation while maintaining a planar base–base arrangement (Figure 4b).

The calculated dG *anti*/*syn* energy differences in the natural deoxydinucleoside monophosphate sequences range from 1.9 to 9.6 kJ mol^{-1} depending on the dG position and the flanking base (Table 3). This range encompasses the *anti*/*syn* energy difference calculated using a nucleotide model (4.8 kJ mol^{-1}).⁵⁶ The energy differences are slightly larger when dG is in the 5' ($6.4\text{--}9.6\text{ kJ mol}^{-1}$) compared with the 3' ($1.9\text{--}5.5\text{ kJ mol}^{-1}$) position. This variation may arise due to differences in the local conformation adopted by the deoxydinucleoside monophosphate to accommodate the *syn* conformation. Specifically, the relative base–base orientation is altered in *syn*-3'-dG sequences, which stabilizes the deoxydinucleoside monophosphate by maximizing favorable interactions between dG and the sugar–phosphate backbone while maintaining a backbone conformation similar to that for the corresponding *anti*-dG structure (Figure 4a). In contrast, the backbone in the *syn*-5'-dG sequences distorts to accommodate the guanine ring over the sugar moiety without forming stabilizing backbone–base interactions, which maintains a nearly parallel relative base–base arrangement (Figure 4b). Most importantly, the relative energy calculated for all natural deoxydinucleoside monophosphates correctly predicts that dG preferentially adopts the *anti* conformation regardless of the position or flanking base. This suggests that distortion in neither the relative base–base orientation nor the sugar–phosphate backbone observed in this model is significant enough to stabilize the *syn* conformation of natural dG. The accurate prediction of the experimentally observed structure and preferred *anti* conformation of natural dG further justifies our computational approach and indicates that the same methodology can be confidently applied to the C8-phenoxy-damaged adducts.

Deoxydinucleoside Monophosphates Containing C8-Phenoxyguanine Adducts. The orientations of the *anti* C8-phenoxy adduct nucleobases relative to the sugar moiety (χ , Table 2) fall within the range found in experimental crystal structures of natural B-DNA⁹⁴ regardless of the damage position

Table 2. Average Values of Backbone Torsional Angles (deg) in Deoxydinucleoside Monophosphates Containing Natural dG or a (*ortho* or *para*) C8-Phenoxy Adduct^a

		dG				<i>o</i> -PhOH-dG				<i>p</i> -PhOH-dG			
		<i>anti</i>		<i>syn</i>		<i>anti</i>		<i>syn</i>		<i>anti</i>		<i>syn</i>	
		5'	3'	5'	3'	5'	3'	5'	3'	5'	3'	5'	3'
exptl value ^b													
$\chi_{5'}$	<i>c</i>	248.1	239.1	84.9	231.5	244.8	245.5	86.1	225.1	245.7	233.6	90.8	226.3
$\chi_{3'}$	<i>c</i>	248.0	274.8	254.6	72.2	255.0	252.1	260.5	90.9	250.7	267.3	248.6	87.9
$\gamma_{5'}$	48 ± 11	48.6	50.2	48.4	48.3	54.1	51.1	48.0	48.2	52.7	51.6	48.1	49.1
$\delta_{5'}$	128 ± 13	147.6	145.2	140.9	140.7	86.0	149.1	139.7	142.4	99.0	148.6	140.9	143.8
$\epsilon_{5'}$	184 ± 11	190.0	194.6	158.0	190.6	163.4	201.2	172.3	199.4	167.1	210.5	170.0	199.4
ζ	265 ± 10	276.9	279.0	266.5	276.6	272.4	280.9	266.6	284.0	262.5	289.1	255.9	286.4
α	298 ± 15	294.8	295.7	301.7	300.9	314.0	287.0	303.9	291.8	312.4	282.1	304.2	291.1
$\beta_{3'}$	176 ± 9	166.8	170.2	182.8	171.0	167.6	159.9	170.7	172.6	169.1	163.1	172.4	172.1
$\gamma_{3'}$	48 ± 11	52.9	53.7	62.1	53.3	59.2	55.5	66.3	50.3	58.4	52.1	63.0	51.5
$\delta_{3'}$	128 ± 13	118.3	144.0	148.7	139.3	145.1	91.5	146.7	146.1	145.3	102.5	145.8	145.0
$\epsilon_{3'}$	184 ± 11	185.7	178.4	175.7	177.9	177.0	193.9	176.4	175.8	177.1	190.1	176.2	175.6

^a M06-2X/6-31G(d,p)-optimized geometries. All angles are defined in Figure 2. ^b Taken from ref 85. ^c Average values are $258^\circ \pm 14^\circ$ for purine and $241^\circ \pm 8^\circ$ for pyrimidine nucleobases.

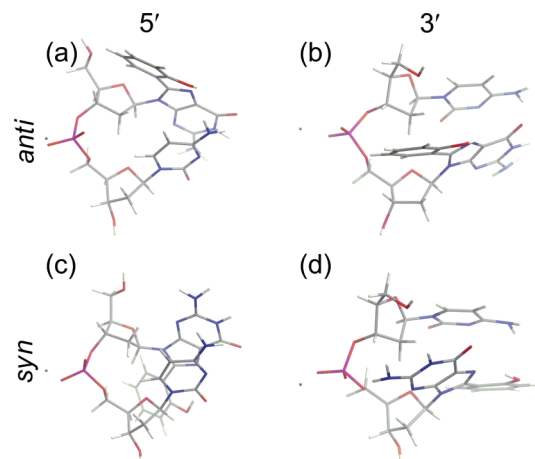
Table 3. M06-2X Relative Energies (kJ mol^{−1}) of the *anti* and *syn* Conformations of dG, as Well as the *o*- or *p*-C8-Phenoxy Adducts, in Deoxydinucleoside Monophosphates^{a,b}

base	position	flanking base							
		cytosine		thymine		adenine		guanine	
		<i>anti</i>	<i>syn</i>	<i>anti</i>	<i>syn</i>	<i>anti</i>	<i>syn</i>	<i>anti</i>	<i>syn</i>
G	5'	0.0	9.6	0.0	7.4	0.0	6.4	0.0	8.6
	3'	0.0	1.9	0.0	5.5	0.0	2.0	0.0	2.2
<i>p</i> -PhOH-G	5'	6.1	0.0	16.1	0.0	0.0	0.1	6.1	0.0
	3'	7.2	0.0	14.4	0.0	21.0	0.0	12.8	0.0
<i>o</i> -PhOH-G	5'	9.2	0.0	16.8	0.0	15.3	0.0	4.8	0.0
	3'	10.9	0.0	15.7	0.0	15.1	0.0	20.8	0.0

^a Relative energies calculated at the M06-2X/6-311+G(2df,p)//M06-2X/6-31G(d,p) level of theory and including scaled (0.9580) ZPVE corrections. ^b Relative energies of the *syn* conformations compared to the *anti* conformations calculated using a nucleotide model are 4.8 kJ mol^{−1} for natural dG, 7.7 kJ mol^{−1} for the *ortho* adduct, and 1.5 kJ mol^{−1} for the *para* adduct. See ref 47.

(5' versus 3') and therefore are very close to those calculated for the corresponding natural sequences, as well as the isolated nucleotide adducts (245–250°).⁵⁶ In contrast, the χ values for the *syn* conformation of the adducts (82–97°, Tables S2 and S3, Supporting Information) are slightly larger than those reported for *syn*-dG (65–89°, Table S1, Supporting Information) for all sequences regardless of the damaged base (*ortho* versus *para*) or position. This agrees with the result for the isolated nucleotide adducts, which have χ angles (81.9–87.9°)⁵⁶ 14–20° greater than that of the *syn*-dG nucleotide (67.9°).⁵⁶ Therefore, the calculated change in χ is likely an inherent property of the bulky adduct regardless of the environment. Nevertheless, it can be concluded that the bulky group does not significantly affect the value of χ for the *anti* or *syn* conformation of natural 2'-deoxyguanosine.

Figures 5 and 6 display examples of optimized deoxydinucleoside monophosphates containing the *o*-PhOH-dG and *p*-PhOH-dG phenoxy adducts, respectively. The natural nucleobases in

**Figure 5.** M06-2X/6-31G(d,p) structure of *o*-PhOH-dG in the 5' (a, c) or 3' (b, d) position and the *anti* (a, b) or *syn* (c, d) conformation with C as the flanking base.

these sequences generally adopt the same orientation observed in the corresponding natural deoxydinucleoside monophosphate and therefore are representative of the conformations in natural B-DNA. However, the orientation of the adduct nucleobase relative to the natural base is somewhat dependent upon the position (5' versus 3'), conformation (*anti* versus *syn*), and isomer (*ortho* versus *para*) of the damage. The unique features of each class of deoxydinucleoside monophosphate will be discussed separately below.

When *anti*-*o*-PhOH-dG is located in the 5' position, the hydroxyl group on the phenoxy ring always forms a (donating or accepting) hydrogen-bonding interaction with the 3' nucleobase (see, for example, Figure 7a). These interactions lead to a greater degree of tilt (ϕ) between the dG component of the adduct and the 3' nucleobase (by 2.5–12.6°, Table 1) compared with that of the corresponding natural strand. Additionally, these structures exhibit a greater degree of twist (θ) about the carbon–carbon bond connecting the phenoxy ring and guanine

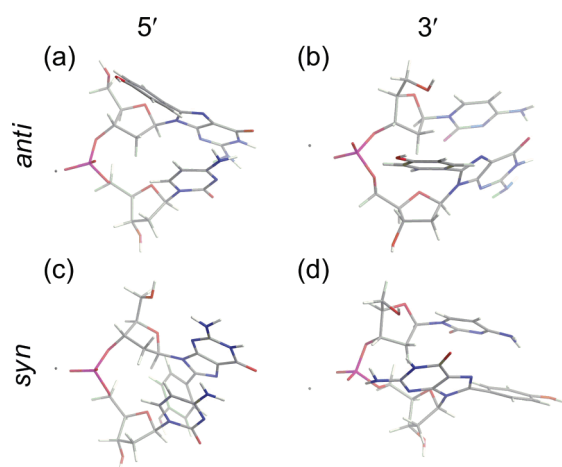


Figure 6. M06-2X/6-31G(d,p) structure of *p*-PhOH-dG in the 5' (a, c) or 3' (b, d) position and the *anti* (a, b) or *syn* (c, d) conformation with C as the flanking base.

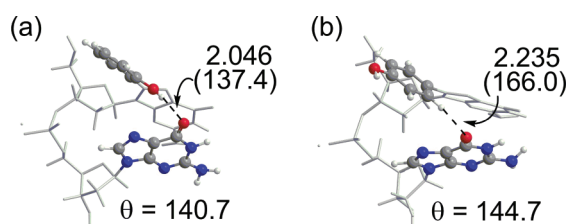


Figure 7. M06-2X/6-31G(d,p) structures (hydrogen bond distances in angstroms, angles in degrees) for the *anti* conformation of (a) *o*-PhOH-dG or (b) *p*-PhOH-dG in the 5' position with G as the 3'-flanking base.

base (by approximately $10\text{--}20^\circ$, Table 1) compared with that of the isolated nucleotide adduct ($\theta = 159.7^\circ$).⁵⁶ Regardless of deviations in θ , the highly stabilizing O–H \cdots N7 intramolecular hydrogen bond that was found in nucleoside⁵⁷ and nucleotide⁵⁶ models is still present when the adduct is incorporated into a deoxydinucleoside monophosphate complex. When the *p*-PhOH-dG adduct is considered in the same position, there are only small variations in θ compared to that of the damaged nucleotide ($\theta = 148.6^\circ$)⁵⁶ when any natural base is in the 3' position (Table 1). Similar θ values coupled with the lack of a strong interaction between the bulky group and the 3' base lead to base–base arrangements comparable to those discussed for the natural sequences involving dT, dC, or dA (Table 1). In contrast, there is a contact between the C–H_{phenyl} of 5'-*p*-PhOH-dG and O6 of 3'-dG (Figure 7b), which leads to a greater base–base tilt as discussed for sequences containing 5'-*o*-PhOH-dG.

The *anti* bulky adduct is subject to more steric crowding when placed in the 3' position. Specifically, close contacts (2.2 Å or less) exist between hydrogen atoms on the phenoxyl ring and those at C2' in the 5' nucleotide for both adducts (Figure 8, left), which may significantly destabilize these configurations. Nevertheless, these arrangements are accompanied by weakly attractive interactions between hydrogen atoms on the phenoxyl group and O5' and/or a phosphate oxygen atom (Figure 8, right). The preferred θ in the *o*-PhOH-dG nucleotide adduct (159.7°)⁵⁶ is not affected by these interactions since the stabilizing O–H \cdots N7 hydrogen bond anchors the relative arrangement of the phenoxyl and guanine rings (Figure 8a, right). However, since

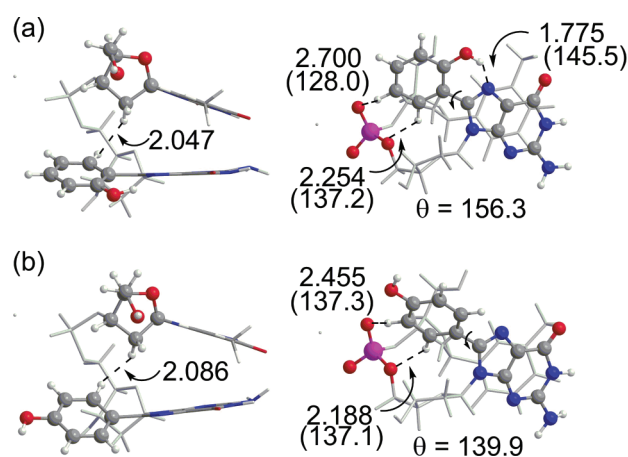


Figure 8. Edge (left) and face (right) views of M06-2X/6-31G(d,p) structures (hydrogen bond distances in angstroms, angles in degrees) for the *anti* conformation of (a) *o*-PhOH-dG or (b) *p*-PhOH-dG in the 3' position with T as the 5'-flanking base.

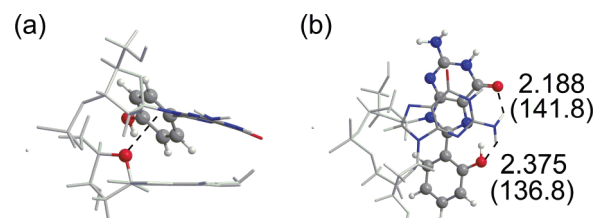


Figure 9. M06-2X/6-31G(d,p) structures (hydrogen bond distances in angstroms, angles in degrees) for the *syn* conformation of (a) *p*-PhOH-dG or (b) *o*-PhOH-dG in the 5' position with G as the 3'-flanking base.

the O–H \cdots N7 interaction is absent in *p*-PhOH-dG (Figure 8b, right), the steric contacts with the phenoxyl group significantly change θ (by up to 21° , Table 1) compared to that of the isolated nucleotide adduct.⁵⁶

Since the phenoxyl group of the *syn* conformation protrudes into the area corresponding to the minor groove of DNA, there is more steric hindrance when this conformation is adopted in the 5' position of a deoxydinucleoside monophosphate compared with that of the *anti* adduct. However, the *syn* conformation leads to O4' lone pair (lp) $\cdots\pi$ interactions with the phenoxyl ring (Figure 9a), which likely provide some stability.⁹⁵ As discussed for the 5' *anti* conformations, the *ortho* adduct exhibits more tilted relative base–base arrangements than the *para* adduct (Table 1). Interactions between the phenoxyl OH group in *o*-PhOH-dG and the 3' nucleobase (i.e., O4 carbonyl of dC or dT, N3 of dA, and N2–H in dG (Figure 9b)) lead to larger deviations (by $2\text{--}35^\circ$) from the preferred θ in the isolated nucleotide ($\theta = 203.4^\circ$, *ortho*; $\theta = 217.1^\circ$, *para*).⁵⁶

Compared with the 5' position, there is less steric crowding between the phenoxyl group and neighboring bases when the *syn* adducts are in the 3' position, and therefore, there are very small changes in the geometry of the adduct nucleotides compared with the isolated counterparts.⁵⁶ Specifically, θ changes by less than 10° for both adducts (Table 1). Most interestingly, the phenoxyl rings of the 3' adducts can participate in stacking interactions with the 5' nucleobase, where ring overlap is more predominant for 5' purines than pyrimidines (Figure 10 a,b).

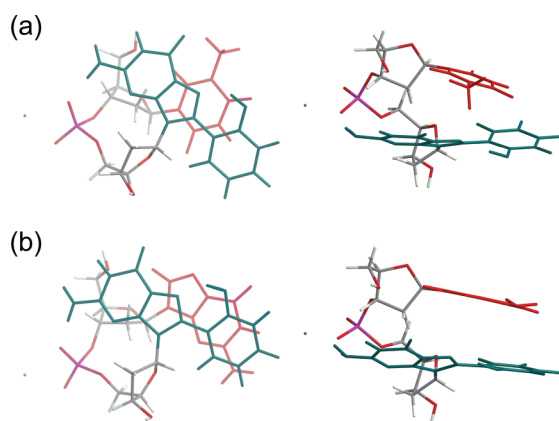


Figure 10. Face (left) and edge (right) views of the stacking interactions between the *syn* conformation of *o*-PhOH-dG (green) and the flanking base (red) when the adduct is in the 3' position and the 5' base is (a) a pyrimidine or (b) a purine.

Since the dG and phenoxyl components of the adducts are twisted relative to one another, the participation of both adduct rings in stacking interactions with the neighboring bases leads to significant tilt for these deoxydinucleoside monophosphate sequences to maximize ring–ring overlap (Table 1).

The backbone angles for the *anti* conformation of the adducts averaged across all sequences are very similar to those found for natural dG (Table 2). The largest changes occur in δ and ϵ when the adduct is in either (5' or 3') position since the sugar puckering changes from C2'-*endo* for natural dG (B-DNA) to C1'-*exo*, O4'-*endo* when the bulky group is positioned above the sugar. Although there are variations in the backbone configuration when the adducts adopt a *syn* versus *anti* conformation, there is less than a 15° distortion in a given backbone dihedral angle when either adduct adopts the *syn* conformation compared to that of the corresponding natural *syn* sequence (Table 2). Therefore, the majority of the distortion in the backbone upon adduct formation is likely due to the induced *syn* conformation of the base rather than the presence of the bulky C8 substituent.

The relative energy between the *anti* and *syn* conformations of the C8-phenoxyl-dG adducts ranges between 0 and 21 kJ mol^{−1} (Table 3). There is no clear correlation between these energy differences and the isomer (*ortho* vs *para*) or position (5' vs 3') of the damage or the nucleobase sequence. However, in contrast to natural dG, both adducts exhibit a preference for the *syn* conformation. Indeed, the *syn* conformer is over 10 kJ mol^{−1} more stable than the corresponding *anti* conformer for the majority of the deoxydinucleoside monophosphates considered. The *syn* conformation of the bulky adducts may be stabilized to a greater extent than the *syn* conformation of natural dG due to the (hydrogen-bonding, stacking) interactions between the phenoxyl group and neighboring nucleotide discussed above. However, the primary reason for the change in the *anti*/*syn* conformational preference upon formation of bulky C8-phenoxyl adducts is likely destabilization of the *anti* conformation due to steric constraints arising from the sheer size of the bulky group and therefore close proximity to the sugar moiety.

The preferential stabilization of the *syn* conformation of the C8-phenoxyl-2'-deoxyguanosine adducts reported here contrasts the conclusion reached when smaller computational models are considered.⁵⁶ Specifically, an isolated nucleotide model predicts the *anti* conformation to be more stable (by 1.5 (*para*) or 7.7

(*ortho*) kJ mol^{−1}),⁵⁶ which contrasts results for C8-methyl-dG^{48,96} or 8-oxoguanine,⁹⁷ where a preference for the *syn* conformation is attributed to steric clashes between the C8 substituent and C2'–H. However, the twist about θ helps relieve the steric clashes in the phenoxyl nucleotide adduct models,⁵⁶ which may explain why the *anti* conformation is not destabilized. When the deoxydinucleoside monophosphate model is considered, similar values of θ likely do not result in relief of steric strain since the twist brings the bulky group of the adduct in the 3' position into close proximity with the sugar of the 5'-flanking residue (Figure 7), while the 5' adducts undergo significant tilt and θ distortions to maintain a stacked alignment with the 3'-flanking base (Figure 6). Furthermore, the magnitude of the difference in relative energies is much larger for the deoxydinucleoside monophosphate systems than calculated using the smaller model. Since deoxydinucleoside monophosphate models are the most relevant to DNA, this emphasizes the importance of using larger models when assessing the *anti*/*syn* preference of bulky DNA adducts, where steric clashes, as well as other (hydrogen-bonding, stacking) interactions, with neighboring bases may dictate the observed conformation.

Since the backbone orientation is proposed to play a role in DNA damage recognition and repair,⁷³ the optimized structures have implications for whether phenoxyl adducts are likely to be recognized by repair enzymes or persist in the helix and potentially lead to mutations.⁷³ Specifically, for other bulky adducts, it has been hypothesized that structural distortions to the helix caused by the *syn* conformation may lead to recognition and repair,^{73,98} while adoption of the *anti* conformation may permit the lesion to go unrecognized (until *anti*/*syn* conversion occurs).⁹⁹ Our calculations suggest that the backbone does not exhibit significant distortion upon adduct formation regardless of the (*anti*/*syn*) conformation adopted, and thus, it is possible that the adduct will not be repaired.

Since the model system implemented in the present work represents the structure of natural DNA duplexes prior to replication,^{53,69} the finding that the *syn* conformation of the adduct is consistently preferred, coupled with our hypothesis that the adduct may not be repaired, has significant implications on the projected mutagenicity of phenolic-mediated damage to guanine. For example, dG-AAF adducts are known to adopt the *syn* conformation,^{54,73} which largely results in frameshift mutations.^{73,100} In contrast, dG-AF adducts, which differ from dG-AAF adducts by only an acetyl group, can adopt either the *anti* or *syn* conformation¹⁰¹ and primarily result in either base-substitution mutations or normal replication.^{21,100} Therefore, if the phenoxyl adducts are primarily in the *syn* conformation, base-substitution mutations or frameshift mutations may arise upon replication.⁵⁵ However, since the relatively small size of the phenoxyl group may not lead to displacement of the base in the complementary strand as seen for larger (AF and AAF) bulky groups, another base may be readily accommodated opposite the adduct and base-substitution mutations may be favored over frameshift mutations.⁷³

To confirm the biological implications of the C8 adduct on the basis of the preferred structures found in this work, future studies must further extend the computational model to DNA duplexes. Indeed, even the structure of the natural deoxydinucleoside monophosphate depends on the location of *syn*-dG, which further suggests both intrastrand neighboring bases could be important for elucidating the adduct structure and *anti*/*syn* energy difference in DNA. Furthermore, differences in the intramolecular contacts when the adducts are located in the 5'

and 3' positions suggest that nucleotides on both sides of the damaged adduct must be simultaneously taken into account. Despite several explicit interactions between the phenoxyl group and the flanking base, the present study finds a lack of sequence dependence on the preferred adduct conformation. Since this contrasts findings for other bulky adducts,^{15,17,102} sequence effects should be further explored in larger DNA duplexes. In particular, DNA duplexes should consider pyrimidine flanking bases simultaneously in the 5' and 3' positions, as well as purines simultaneously in both positions, since these two environments represent the extremes in base–base overlap observed in the current study. While the present work suggests intrastrand base–base and backbone interactions lead to a preference for the *syn* conformation, previous studies have found that complementary base-pairing with the adducts is stronger in the *anti* conformation.⁵⁹ In addition, discrete interactions between the phenoxyl moiety and flanking bases may affect the adduct hydrogen-bonding patterns¹⁰³ and therefore its base-pairing preference.⁵⁹ Therefore, simulations of DNA duplexes with the adducts paired with the strongest (cytosine and guanine)⁵⁹ binding partners for each (*anti* and *syn*) conformation are necessary to determine the most likely conformations and hydrogen-bonding patterns adopted by the adducts in biological systems. These models will allow us to consider the combined effects of stacking and hydrogen-bonding on the conformational and base-pairing preference of these important DNA adducts.

CONCLUSIONS

The dG component of the bulky *o*- and *p*-C8-phenoxyl nucleotide adducts assumes a relative base–base orientation and backbone conformation similar to those of the corresponding natural nucleotide in a deoxydinucleoside monophosphate model. However, the conformation of the C8-phenoxyl group can be characterized according to the position (5' versus 3'), conformation (*anti* versus *syn*), and isomer (*ortho* versus *para*) of the damage. While the *ortho* adduct has greater conformational flexibility since the hydroxyl group can interact with neighboring bases and thereby cause distortion to the local structure, the *para* adduct is relatively unaffected by these considerations.

The most striking conclusion is the change in relative energies of the *anti* and *syn* conformations upon DNA damage. In particular, when the adduct is in the 3' position, the *anti* conformation is destabilized by steric clashes between the phenoxyl group and the 5' sugar, as well as the phosphate backbone. Although there is often a high degree of tilt when the adduct is in the 5' position to maintain stabilizing interactions with the 3'-flanking base, these interactions are insufficient to overcome destabilization due to the steric clash between the bulky group and the sugar. In the *syn* conformation, overlap with the flanking base is enhanced with respect to *syn* natural dG due to the involvement of the phenoxyl ring, especially when the adduct is in the 3' position. In the 5' position, the phenoxyl ring of the adduct forms $\text{lp} \cdots \pi$ interactions with O4' of the 3'-flanking base. Therefore, while natural dG exhibits a clear preference for the *anti* conformation, addition of the bulky C8-phenoxyl group results in a preference for the *syn* conformation regardless of the sequence or position.

Since the findings in the present work differ from those previously reported using smaller models (nucleoside, nucleotide),⁵⁶ our work stresses the importance of using models that address both base–base and backbone interactions when determining the conformational preferences of bulky adducts.

Furthermore, since replication errors for other C8 bulky adducts have been proposed to result from a *syn* conformational preference, our findings provide clues to the possible mutagenicity of phenolic adducts. Future work must expand the model system to determine the effects of simultaneous interactions with both the 5'- and 3'-flanking bases and hydrogen-bonding and steric interactions with the complementary strand, as well as determine whether mismatches can be stabilized. Molecular dynamics simulations are currently under way in our laboratory to incorporate all of the above structural influences into a single system that will increase our understanding of the conformational and base-pairing properties of phenoxyl DNA damage.

ASSOCIATED CONTENT

S Supporting Information. Backbone torsion angles for all dinucleoside monophosphates (Tables S1–S3). This material is available free of charge via the Internet at <http://pubs.acs.org>. Cartesian coordinates of the calculated structures are available upon request.

AUTHOR INFORMATION

Corresponding Author

*E-mail: stacey.wetmore@uleth.ca.

Author Contributions

[§]These authors contributed equally to this work.

ACKNOWLEDGMENT

We thank the Canada Foundation for Innovation (CFI), the Natural Sciences and Engineering Research Council (NSERC), and the Canada Research Chair program for financial support. We acknowledge the Upscale and Robust Abacus for Chemistry in Lethbridge (URACIL) for computer resources. F.M.V.L. and B.L.K. thank the NSERC for undergraduate (USRA) research awards, and A.L.M. thanks the NSERC (CGS-D) and Alberta Innovates-Technology Futures for student scholarships.

REFERENCES

- (1) Geacintov, N. E.; Broyde, S., Eds. *The Chemical Biology Of DNA Damage*; Wiley-VCH Verlag GmbH & Co. KGaA: Weinheim, Germany, 2010.
- (2) Halliwell, B. *J. Neurochem.* **2006**, 97, 1634–1658.
- (3) Nakabeppu, Y.; Tsuchimoto, D.; Yamaguchi, H.; Sakumi, K. *J. Neurosci. Res.* **2007**, 85, 919–934.
- (4) Lu, A. L.; Li, X.; Gu, Y.; Wright, P. M.; Chang, D.-Y. *Cell Biochem. Biophys.* **2001**, 35, 141–170.
- (5) Labahn, J.; Scharer, O. D.; Long, A.; EzazNikpay, K.; Verdine, G. L.; Ellenberger, T. E. *Cell* **1996**, 86, 321–329.
- (6) Drablos, F.; Feyzi, E.; Aas, P. A.; Vaagbo, C. B.; Kavli, B.; Bratlie, M. S.; Pena-Diaz, J.; Otterlei, M.; Slupphaug, G.; Krokan, H. E. *DNA Repair* **2004**, 3, 1389–1407.
- (7) Gates, K. S.; Noonan, T.; Dutta, S. *Chem. Res. Toxicol.* **2004**, 17, 839–856.
- (8) Kow, Y. W. *Free Radical Biol. Med.* **2002**, 33, 886–893.
- (9) Labet, V.; Grand, A.; Morell, C.; Cadet, J.; Eriksson, L. A. *Theor. Chem. Acc.* **2008**, 120, 429–435.
- (10) Bloomfield, V. A.; Crothers, D. M.; Tinoco, I., Jr. *Nucleic Acids Structures, Properties, and Functions*; University Science Press: Mill Valley, CA, 2000.
- (11) Dai, J.; Wright, M. W.; Manderville, R. A. *Chem. Res. Toxicol.* **2003**, 16, 817–821.

- (12) Dai, J.; Wright, M. W.; Manderville, R. A. *J. Am. Chem. Soc.* **2003**, *125*, 3716–3717.
- (13) Gannett, P. M.; Lawson, T.; Miller, M.; Thakkar, D. D.; Lord, J. W.; Yau, W. M.; Toth, B. *Chem.-Biol. Interact.* **1996**, *101*, 149–164.
- (14) Stover, J. S.; Ciobanu, M.; Cliffl, D. E.; Rizzo, C. J. *J. Am. Chem. Soc.* **2007**, *129*, 2074–2081.
- (15) Elmquist, C. E.; Wang, F.; Stover, J. S.; Stone, M. P.; Rizzo, C. J. *Chem. Res. Toxicol.* **2007**, *20*, 445–454.
- (16) Cho, B. P.; Beland, F. A.; Marques, M. M. *Biochemistry* **1992**, *31*, 9587–9602.
- (17) Jain, N.; Meneni, S.; Jain, V.; Cho, B. P. *Nucleic Acids Res.* **2009**, *37*, 1628–1637.
- (18) Liang, F. T.; Meneni, S.; Cho, B. P. *Chem. Res. Toxicol.* **2006**, *19*, 1040–1043.
- (19) Yang, Z. Z.; Qi, S. F.; Zhao, D. X.; Gong, L. D. *J. Phys. Chem. B* **2009**, *113*, 254–259.
- (20) Broyde, S.; Wang, L. H.; Zhang, L.; Rechakoblit, O.; Geacintov, N. E.; Patel, D. J. *Chem. Res. Toxicol.* **2008**, *21*, 45–52.
- (21) Cho, B. S. P. *J. Environ. Sci. Health, Part C: Environ. Carcinog. Ecotoxicol. Rev.* **2004**, *22*, 57–90.
- (22) Dai, Q.; Xu, D. W.; Lim, K.; Harvey, R. G. *J. Org. Chem.* **2007**, *72*, 4856–4863.
- (23) Lakshman, M. K.; Keeler, J. C.; Ngassa, F. N.; Hilmer, J. H.; Pradhan, P.; Zajc, B.; Thomasson, K. A. *J. Am. Chem. Soc.* **2007**, *129*, 68–76.
- (24) Huang, X. W.; Colgate, K. C.; Kolbanovskiy, A.; Amin, S.; Geacintov, N. E. *Chem. Res. Toxicol.* **2002**, *15*, 438–444.
- (25) Jin, B.; Lee, H. M.; Kim, S. K. *J. Biomol. Struct. Dyn.* **2010**, *27*, 457–464.
- (26) Pfohl-Leszkowicz, A.; Manderville, R. A. *Mol. Nutr. Food Res.* **2007**, *51*, 61–99.
- (27) Tozlovanu, M.; Faucet-Marquis, V.; Pfohl-Leszkowicz, A.; Manderville, R. A. *Chem. Res. Toxicol.* **2006**, *19*, 1241–1247.
- (28) Dai, J.; Sloat, A. L.; Wright, M. W.; Manderville, R. A. *Chem. Res. Toxicol.* **2005**, *18*, 771–779.
- (29) Kato, T.; Kojima, K.; Hiramoto, K.; Kikugawa, K. *Mutat. Res.* **1992**, *268*, 105–114.
- (30) Calcutt, M. W.; Gillman, I. G.; Nofle, R. E.; Manderville, R. A. *Chem. Res. Toxicol.* **2001**, *14*, 1266–1272.
- (31) Manderville, R. A. *Can. J. Chem./Rev. Can. Chim.* **2005**, *83*, 1261–1267.
- (32) Kikugawa, K.; Kato, T.; Kojima, K. *Mutat. Res.* **1992**, *268*, 65–75.
- (33) Hiramoto, K.; Kojima, K.; Kato, T.; Kikugawa, K. *Mutat. Res.* **1992**, *272*, 259–260.
- (34) Guengerich, F. P.; Mundkowski, R. G.; Voehler, M.; Kadlubar, F. F. *Chem. Res. Toxicol.* **1999**, *12*, 906–916.
- (35) Kennedy, S. A.; Novak, M.; Kolb, B. A. *J. Am. Chem. Soc.* **1997**, *119*, 7654–7664.
- (36) McClelland, R. A.; Ahmad, A.; Dicks, A. P.; Licence, V. E. *J. Am. Chem. Soc.* **1999**, *121*, 3303–3310.
- (37) Qi, S.-F.; Wang, X.-N.; Yang, Z.-Z.; Xu, X.-H. *J. Phys. Chem. B* **2009**, *113*, 5645–5652.
- (38) Qi, S.-F.; Wang, X.-N.; Yang, Z.-Z.; Xu, X.-H. *Comput. Theor. Chem.* **2011**, *965*, 84–91.
- (39) Qi, S.-F.; Yang, Z.-Z. *J. Org. Chem.* **2007**, *72*, 10058–10064.
- (40) Shi-Fei, Q. I.; Xiao-Nan, W.; Zhong-Zhi, Y. *J. Theor. Comput. Chem.* **2009**, *8*, 1053–1071.
- (41) Yang, Z.-Z.; Qi, S.-F. *J. Phys. Chem. B* **2007**, *111*, 13444–13450.
- (42) Yang, Z.-Z.; Qi, S.-F.; Zhao, D.-X.; Gong, L.-D. *J. Phys. Chem. B* **2008**, *113*, 254–259.
- (43) Kreutzer, D. A.; Essigmann, J. M. *Proc. Natl. Acad. Sci. U.S.A.* **1998**, *95*, 3578–3582.
- (44) Wallace, S. S. *Free Radical Biol. Med.* **2002**, *33*, 1–14.
- (45) Cai, Y.; Patel, D. J.; Geacintov, N. E.; Broyde, S. J. *Mol. Biol.* **2007**, *374*, 292–305.
- (46) Eason, R. G.; Burkhardt, D. M.; Phillips, S. J.; Smith, D. P.; David, S. S. *Nucleic Acids Res.* **1996**, *24*, 890–897.
- (47) Heavner, S.; Gannett, P. M. *J. Biomol. Struct. Dyn.* **2005**, *23*, 203–219.
- (48) Vongsutilers, V.; Phillips, D. J.; Train, B. C.; McKelvey, G. R.; Thomsen, N. M.; Shaughnessy, K. H.; Lewis, J. P.; Gannett, P. M. *Biophys. Chem.* **2011**, *154*, 41–48.
- (49) Burnouf, D. Y.; Wagner, J. E. *J. Mol. Biol.* **2009**, *386*, 951–961.
- (50) Hilario, P.; Yan, S. X.; Hingerty, B. E.; Broyde, S.; Basu, A. K. *J. Biol. Chem.* **2002**, *277*, 45068–45074.
- (51) Watt, D. L.; Utzat, C. D.; Hilario, P.; Basu, A. K. *Chem. Res. Toxicol.* **2007**, *20*, 1658–1664.
- (52) Donny-Clark, K.; Shapiro, R.; Broyde, S. *Biochemistry* **2009**, *48*, 7–18.
- (53) Shapiro, R.; Sidawi, D.; Miao, Y. S.; Hingerty, B. E.; Schmidt, K. E.; Moskowitz, J.; Broyde, S. *Chem. Res. Toxicol.* **1994**, *7*, 239–253.
- (54) Wang, L. H.; Broyde, S. *Nucleic Acids Res.* **2006**, *34*, 785–795.
- (55) Liang, F. T.; Cho, B. P. *Chem. Res. Toxicol.* **2011**, *24*, 597–605.
- (56) Millen, A. L.; Manderville, R. A.; Wetmore, S. D. *J. Phys. Chem. B* **2010**, *114*, 4373–4382.
- (57) Millen, A. L.; McLaughlin, C. K.; Sun, K. M.; Manderville, R. A.; Wetmore, S. D. *J. Phys. Chem. A* **2008**, *112*, 3742–3753.
- (58) Schlitt, K. M.; Sun, K. W. M.; Paugh, R. J.; Millen, A. L.; Navarro-Whyte, L.; Wetmore, S. D.; Manderville, R. A. *J. Org. Chem.* **2009**, *74*, 5793–5802.
- (59) Millen, A. L.; Churchill, C. D. M.; Manderville, R. A.; Wetmore, S. D. *J. Phys. Chem. B* **2010**, *114*, 12995–13004.
- (60) Jia, L.; Shafirovich, V.; Shapiro, R.; Geacintov, N. E.; Broyde, S. *Biochemistry* **2006**, *45*, 6644–6655.
- (61) Shapiro, R.; Hingerty, B. E.; Broyde, S. J. *Biomol. Struct. Dyn.* **1989**, *7*, 493–513.
- (62) Norman, D.; Abuaf, P.; Hingerty, B. E.; Live, D.; Grunberger, D.; Broyde, S.; Patel, D. J. *Biochemistry* **1989**, *28*, 7462–7476.
- (63) Cho, B. P.; Beland, F. A.; Marques, M. M. *Biochemistry* **1994**, *33*, 1373–1384.
- (64) Eckel, L. M.; Krugh, T. R. *Nat. Struct. Biol.* **1994**, *1*, 89–94.
- (65) Eckel, L. M.; Krugh, T. R. *Biochemistry* **1994**, *33*, 13611–13624.
- (66) Poltev, V. I.; Anisimov, V. M.; Danilov, V. I.; Deriabina, A.; Gonzalez, E.; Jurkiewicz, A.; Les, A.; Polteva, N. *J. Biomol. Struct. Dyn.* **2008**, *25*, 563–571.
- (67) Poltev, V. I.; Anisimov, V. M.; Danilov, V. I.; Deriabina, A.; Gonzalez, E.; Garcia, D.; Rivas, F.; Jurkiewicz, A.; Les, A.; Polteva, N. *J. Mol. Struct.: THEOCHEM* **2009**, *912*, 53–59.
- (68) Poltev, V. I.; Anisimov, V. M.; Danilov, V. I.; Mourik, T. v.; Deriabina, A.; Gonzalez, E.; Padua, M.; Garcia, D.; Rivas, F.; Polteva, N. *Int. J. Quantum Chem.* **2010**, *110*, 2548–2559.
- (69) Hingerty, B.; Broyde, S. *Biochemistry* **1982**, *21*, 3243–3252.
- (70) Meneni, S. R.; Shell, S. M.; Gao, L.; Jurecka, P.; Lee, W.; Sponer, J.; Zou, Y.; Chiarelli, M. P.; Cho, B. P. *Biochemistry* **2007**, *46*, 11263–11278.
- (71) Meneni, S.; Shell, S. M.; Zou, Y.; Cho, B. P. *Chem. Res. Toxicol.* **2007**, *20*, 6–10.
- (72) Mao, B.; Hingerty, B. E.; Broyde, S.; Patel, D. J. *Biochemistry* **1998**, *37*, 95–106.
- (73) Patel, D. J.; Mao, B.; Gu, Z. T.; Hingerty, B. E.; Gorin, A.; Basu, A. K.; Broyde, S. *Chem. Res. Toxicol.* **1998**, *11*, 391–407.
- (74) Gu, Z. T.; Gorin, A.; Hingerty, B. E.; Broyde, S.; Patel, D. J. *Biochemistry* **1999**, *38*, 10855–10870.
- (75) Tereshko, V.; Minasov, G.; Egli, M. *J. Am. Chem. Soc.* **1999**, *121*, 470–471.
- (76) Gorb, L.; Shishkin, O.; Leszczynski, J. *J. Biomol. Struct. Dyn.* **2005**, *22*, 441–454.
- (77) Kosenkov, D.; Gorb, L.; Shishkin, O. V.; Sponer, J.; Leszczynski, J. *J. Phys. Chem. B* **2008**, *112*, 150–157.
- (78) Kosenkov, D.; Kholod, Y. A.; Gorb, L.; Shishkin, O. V.; Kuramshina, G. M.; Dovbeshko, G. I.; Leszczynski, J. *J. Phys. Chem. A* **2009**, *113*, 9386–9395.
- (79) Leulliot, N.; Ghomi, M.; Scalmani, G.; Berthier, G. *J. Phys. Chem. A* **1999**, *103*, 8716–8724.
- (80) Palamarchuk, G. V.; Shishkin, O. V.; Gorb, L.; Leszczynski, J. *J. Biomol. Struct. Dyn.* **2009**, *26*, 653–661.

- (81) Rubio, M.; Roca-Sanjuan, D.; Serrano-Andres, L.; Merchan, M. *J. Phys. Chem. B* **2009**, *113*, 2451–2457.
- (82) Shishkin, O. V.; Gorb, L.; Zhikol, O. A.; Leszczynski, J. *J. Biomol. Struct. Dyn.* **2004**, *21*, 537–553.
- (83) Shishkin, O. V.; Gorb, L.; Zhikol, O. A.; Leszczynski, J. *J. Biomol. Struct. Dyn.* **2004**, *22*, 227–243.
- (84) Shishkin, O. V.; Palamarchuk, G. V.; Gorb, L.; Leszczynski, J. *J. Phys. Chem. B* **2006**, *110*, 4413–4422.
- (85) Sponer, J.; Sabat, M.; Gorb, L.; Leszczynski, J.; Lippert, B.; Hobza, P. *J. Phys. Chem. B* **2000**, *104*, 7535–7544.
- (86) Svozil, D.; Šponer, J. E.; Marchan, I.; Pérez, A.; Cheatham, T. E., III; Forti, F.; Luque, F. J.; Orozco, M.; Šponer, J. *J. Phys. Chem. B* **2008**, *112*, 8188–8197.
- (87) Zakrevskii, V. V.; Dolgounitcheva, O.; Zakrzewski, V. G.; Ortiz, J. V. *Int. J. Quantum Chem.* **2007**, *107*, 2266–2273.
- (88) Scalmani, G.; Frisch, M. J. *J. Chem. Phys.* **2010**, *132*, 114110–114115.
- (89) Dąbkowska, I.; Gonzalez, H. V.; Jurečka, P.; Hobza, P. *J. Phys. Chem. A* **2005**, *109*, 1131–1136.
- (90) Zhao, Y.; Truhlar, D. G. *Theor. Chem. Acc.* **2008**, *120*, 215–241.
- (91) Merrick, J. P.; Moran, D.; Radom, L. *J. Phys. Chem. A* **2007**, *111*, 11683–11700.
- (92) Frisch, M. J.; Trucks, G. W.; Schlegel, H. B.; Scuseria, G. E.; Robb, M. A.; Cheeseman, J. R.; Scalmani, G.; Barone, V.; Mennucci, B.; Petersson, G. A.; Nakatsuji, H.; Caricato, M.; Li, X.; Hratchian, H. P.; Izmaylov, A. F.; Bloino, J.; Zheng, G.; Sonnenberg, J. L.; Hada, M.; Ehara, M.; Toyota, K.; Fukuda, R.; Hasegawa, J.; Ishida, M.; Nakajima, T.; Honda, Y.; Kitao, O.; Nakai, H.; Vreven, T.; Jr., J. A. M.; Peralta, J. E.; Ogliaro, F.; Bearpark, M.; Heyd, J. J.; Brothers, E.; Kudin, K. N.; Staroverov, V. N.; Kobayashi, R.; Normand, J.; Raghavachari, K.; Rendell, A.; Burant, J. C.; Iyengar, S. S.; Tomasi, J.; Cossi, M.; Rega, N.; Millam, J. M.; Klene, M.; Knox, J. E.; Cross, J. B.; Bakken, V.; Adamo, C.; Jaramillo, J.; Gomperts, R.; Stratmann, R. E.; Yazyev, O.; Austin, A. J.; Cammi, R.; Pomelli, C.; Ochterski, J. W.; Martin, R. L.; Morokuma, K.; Zakrzewski, V. G.; Voth, G. A.; Salvador, P.; Dannenberg, J. J.; Dapprich, S.; Daniels, A. D.; Farkas, O.; Foresman, J. B.; Ortiz, J. V.; Cioslowski, J.; Fox, D. J. *Gaussian 09*, revision A.02; Gaussian, Inc.: Wallingford, CT, 2009.
- (93) Saenger, W. *Principles of Nucleic Acid Structure*; Springer-Verlag New York Inc.: New York, 1984.
- (94) Schneider, B.; Neidle, S.; Berman, H. M. *Biopolymers* **1997**, *42*, 113–124.
- (95) Egli, M.; Sarkhel, S. *Acc. Chem. Res.* **2007**, *40*, 197–205.
- (96) Kohda, K.; Tsunomoto, H.; Minoura, Y.; Tanabe, K.; Shibutani, S. *Chem. Res. Toxicol.* **1996**, *9*, 1278–1284.
- (97) Gannett, P. M.; Sura, T. P. *Chem. Res. Toxicol.* **1993**, *6*, 690–700.
- (98) Geacintov, N. E.; Broyde, S.; Buterin, T.; Naegeli, H.; Wu, M.; Yan, S. X.; Patel, D. J. *Biopolymers* **2002**, *65*, 202–210.
- (99) Perlow, R. A.; Broyde, S. *J. Mol. Biol.* **2002**, *322*, 291–309.
- (100) Bichara, M.; Fuchs, R. P. P. *J. Mol. Biol.* **1985**, *183*, 341–351.
- (101) Mao, B.; Hingerty, B. E.; Broyde, S.; Patel, D. J. *Biochemistry* **1998**, *37*, 81–94.
- (102) Wang, F.; Elmquist, C. E.; Stover, J. S.; Rizzo, C. J.; Stone, M. P. *Biochemistry* **2007**, *46*, 8498–8516.
- (103) Dupradeau, F. Y.; Case, D. A.; Yu, C. Z.; Jimenez, R.; Romesberg, F. E. *J. Am. Chem. Soc.* **2005**, *127*, 15612–15617.